JCRS

Journal of Chemical Reactivity and Synthesis 2024:14(2) 111-126

Research Article

Study and determine the isotherm of Metronidazole absorption with new Co-MOF nanostructure $[[Co_2(TATAB)(OH)(H_2O)_2].H_2O.0.6O]_n$

Seyedeh Elahe Hosseini [1], Mohammad Kazem Mohammadi[1*], Ayeh Rayatzadeh,[1]

Haman Tavakkoli [1], Payam Hayati [2]

[1] Department of Chemistry, Ahvaz Branch, Islamic Azad University, Ahvaz, Iran.

[2] Organic and Nano Group, Department of Chemistry, Iran University of Science and Technology, 16846-13114 Tehran, Iran.

ARTICLE INFO:

Received:
6 January 2025

Accepted:
27 February 2025

Available online:
28 February 2025

✉: M.K.Mohammadi
mkmohamadi@gmail.com

ABSTRACT

The simple chemical synthesis method was used for the preparation of nano Co-MOF nanostructures. In this study, Co-MOF nanostructure was presented as a good, natural, and inexpensive adsorbent and successfully used for the removal of metronidazole dyes from various water solutions. The structural functionalities and morphological observations were confirmed by FESEM- XRD- FTIR- EDS- TEM.

In this research, the effect of various parameters such as pH, dye concentration, amount of adsorbent, contact time, and temperature on the removal process for metronidazole was investigated. The adsorption process was dependent on pH, initial dye concentration, adsorbent dose, contact time, and temperature. The maximum removal was 99.5 % under optimal conditions. The isothermal adsorption data could be interpreted by the isothermal models of Langmuir and Freundlich. The experimental data agreed with Freundlich's adsorption isotherms. Optimized values for metronidazole removal were pH: 9, contact time: 120 minutes, dye concentration: 10 mg/ l, and catalyst mass: 0.04 g. Under these optimal conditions, the maximum removal efficiency reached 99.5%.

Keywords: Adsorption; Metronidazole; Co-MOF; Removal; Isotherm

1. Introduction

Due to its complexity, water pollution from the dyeing of textile fibers, paper, leather, plastics, and pharmaceuticals is one of the most difficult problems in industrial waste management that has a direct impact on drinking water [1, 2]. They are significant pollutants that cause environmental and health problems [3]. Most of them are toxic and even carcinogenic, posing a serious risk to humans and aquatic animals [4]. A large number of dyes are commercially available and used in many industries, e.g. textile, printing, paper, and plastics [5, 6].

Colorants have a considerable structural diversity and are classified in different ways. Aromatic food dyes are the largest category of synthetic dyes and are characterized by the presence of one or more aromatic systems, which may also contain sulfonic acid or other substitution groups. Metronidazole is a water-soluble, cherry-red, synthetic carbon dye of the xanthene class that is used to dye various materials such as wool, silk, and nylon. It is one of the most commonly used dyes in pharmaceuticals and cosmetics [7]. It is also used to color a variety of foods, such as cocktail drinks, canned cherries, fruit, cookies, chocolate, crabmeat, salmon spread, stuffed olives, candy, baked goods, snacks, chewing gum, jelly, ice cream, etc. [8].

Metronidazole is a synthetic azo dye that gives food a red color. This colorant is used in foods such as jelly, jam, sweets, and preservatives. The use of metronidazole is banned in many industrialized countries because it contains b-naphthylamine, a known carcinogen produced by the reduction of azo groups. [9] Therefore, it is necessary to focus research on the removal of metronidazole from wastewater by using an applicable method without by-products. [10, 11]

Activated carbon is undoubtedly considered a universal adsorbent for wastewater treatment and is often used for the removal of various pollutants such as organic dyes [12]. However,

its extensive use in wastewater treatment is sometimes limited due to its higher cost. Some methods are used for wastewater treatment. Among others, different types of non-conventional sorbents have been studied for their ability to remove various types of pollutants from wastewater. [13]

MOF are highly porous hydrated aluminum silicate materials with three-dimensional crystal structures. There are more than 40 natural zeolites worldwide [13]. MOF are used in many areas, e.g. as building blocks, cement, pozzolan, and lightweight aggregates, for the removal of oil spills, as paper filler and desiccant, and for the separation of gasses and liquids [14]. They have also been extensively studied for their applicability in the removal of pollutants such as heavy metal ions, ammonium, inorganic anions, phenols, pesticides, and dyes in water, [15]. The high ion exchange capacity, the relatively large specific surface area and, above all, the relatively low cost make zeolites attractive adsorbents [16]. However, the adsorption of anionic reactive dyes with MOF is very limited due to the surface area of the MOF and the negatively charged dye molecules [17, 18].

2. Experimental

2.1 Materials

All compounds and solvents were sourced from Sigma-Aldrich and used as received without any additional modifications. Various equipment and instruments were employed for compound analysis as follows: A JASCO 680-PLUS spectrometer was used to generate FT-IR spectra. Elemental analysis was performed using a Heraeus Analytical Jena Multiple EA 3100 CHNO instrument. X-ray powder diffraction measurements were conducted using a Philips X'pert diffractometer and monochromatized CuKα radiation. The HITACHI S-3700N Scanning Electron Microscope (SEM) was utilized to assess the size and shape of the compounds. A Scientz- SB-120D ultrasonic bath was used for the fabrication of both nano

and macro-scale compounds. The determination of melting points was carried out using a Buchi M-565 model equipment. For the single crystal structure of compound 1, data was collected using a STOE-IPDS II diffractometer with MoKα radiation at 173(2) K. Data reduction and semi-experimental absorption correction were performed using the SADABS program .The structure of compound 1 was determined using robust methods (SIR97 program and subsequently refined based on the F_2 values with Olix and SHELEX-2018/8 software , with the aid of the WinGX program . Hydrogen atoms attached to carbon atoms were generated according to stereochemical principles and refined using the riding model. After incorporating carbon-bound and hydrogen atoms, the bonded oxygen atoms were utilized as starting maxima for Fourier maps, and their coordinates were refined with various restraints on bond lengths. Hirschfeld surface analysis (HSA) was performed using CrystalExplorer17 software. Powder XRD patterns were generated through simulation using Mercury software, using single crystal data. For additional details concerning data collection parameters, final refinement, and crystallographic data, please consult the supplementary material. You can find selected geometric parameters in Tables S1 and 1.

2.2. Ultrasonic Synthesis of Compound 1 in Powder Form

To obtain compound 1 in powdered form, the following procedure was executed: The probe of the ultrasonic device was immersed in a solution containing Co $(NO_3)_2 \cdot 6H_2O$ (10 mL, 0.1 M) and H_3TATAB (10 mL, 0.1 M) was gradually added. This experiment was performed five times to investigate the effect of different factors on the resulting powders. Factors such as reaction time, temperature, reactant concentration and ultrasonic power were tested, the details of which are given in Table 1. After each experiment, the obtained powders were subjected to filtration, washing with distilled water and drying for further analysis.

Elemental analysis for $Co_2C_{24}H_{22}N_6O_{10.6}$: Calculated for C, 0.42; H, 0.03; N, 0.12. Found: C, 0.34; H, 0.02; N, 0.10%. Infrared spectroscopy (IR) was conducted, with selected bands for

compound 1 recorded at the following wavenumbers in cm^{-1}: 3350 (s), 2987 (b), 1762 (s), 1236 (w).

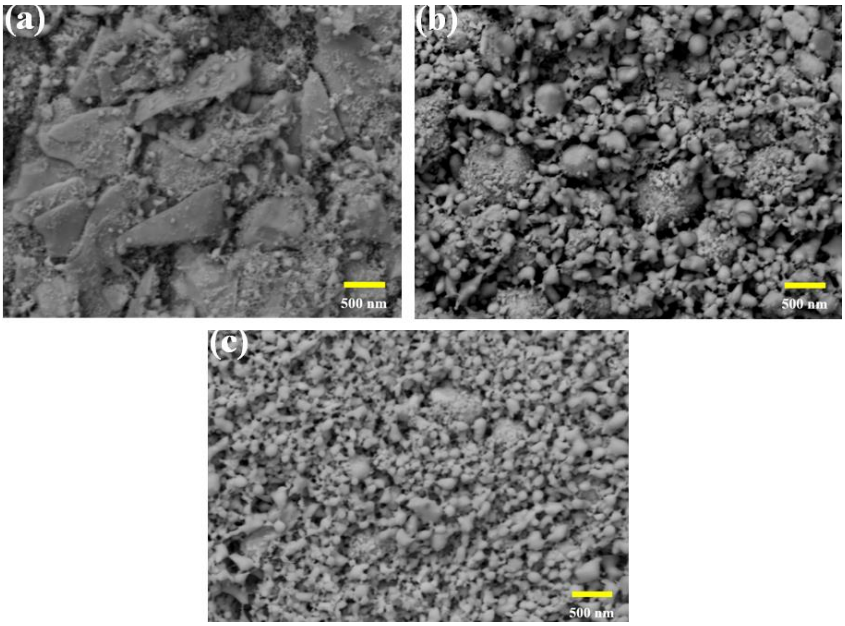

Fig. 1. SEM images and the corresponding particle size: (**a**) 1-1 by sonochemical reaction (50 °C, 60 min reaction time, concentration of reactants 0.1 M, 60 W power), (**b**) 1-2 same as (**a**) but 30 min reaction time, (**c**) 1-3 same as (**a**) but at 70

2.3 Dye removal

Physical adsorption is based on weak intermolecular interactions, while chemisorption is based on the exchange of valence electrons between the adsorbent and the adsorbate. It is not always possible to define the boundary between physisorption and chemisorption. Observing the adsorption of metronidazole on nanostructure can provide interesting information about possible interactions with the zeolite surface. It is assumed that nanostructure was the worst adsorbent for these dyes. The results obtained can be explained by the fact that the acidity of the surface was decisive for the adsorption, i.e. the presence of active Lewis and Brønsted centers on the outer and inner nanostructure surfaces.

A comparison between some zeolite-modified structures for different dyes is shown in Table 1.

Table 1. Comparison between some adsorbents for dye removal

Adsorbent	Dye/textile wastewater	Initial concentration	Dye/ color removal	Contact time	pH	Source
nanocomposites-based cellulose derivatives-$CuFe_2O_4$-zeolite	Brilliant Green	8.56 ×10-5 mol/L	99%	120 min	5	[19]
CWPO/ Fe- zeolite	azo dye (Congo red)		100%	4 h	7	[20]
Fe–Zn bimetallic nanoparticles supported by hydroxyethyl cellulose/graphene oxide	doxycycline	100 mg/l	97%	90 min	2.5	[21]
AOPs/Fe ZMS-5 zeolite	Reactive Brilliant Blue KN-R	250-500 mg/l	95%	90 min	2.5	[22]
activated clay-ZnO	Maxilon red	100 mg/l	80%	1 h	10.8	[23]
Zn/Si	methylene blu	20-100 ppm	87%	5 h	9-11	[24]
O_3/zeolite	Methylene blue (MB)	30 mg/l	25%	24 h	2-8	[25]

2.4 Calibration of Metronidazole

To calibrate the concentration of the dye solutions, we created a calibration curve of the dyes metronidazole. Therefore, the concentration of the dye samples could be calculated from the corresponding maximum absorbance values. The calibration curves are shown in Fig. (2). To ensure the accuracy of the absorbance measurement, the dye concentration was limited to 25 mg/l. Each dye solution (250 ml) was stored in the dark to avoid any oxidation. The stirrer speed, pH, and temperature were kept constant during all experiments. The efficiency of dye removal was determined over 180 minutes. The multiple absorbances of each sample were recorded at selected wavelengths and the average values were reported.

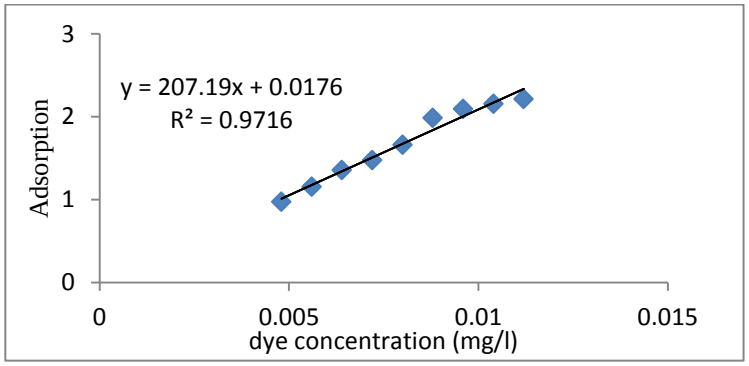

Fig .2: Calibration Curve of Metronidazole

The concentration of Metronidazole could be calculated from related maximum absorbance values.

3. Result and discussion

3.1 Dyes Removal Studies

The behavior and performance of a nanostructure for dye removal were studied using 250 mL of each dye solution with specific initial concentrations, pH levels, contact times, and nanostructure dosages in a reaction system. [26]

3.2 Effect of pH

The impact of pH on the removal of metronidazole was assessed using a Nanocomposite as an absorbent across various pH levels (3, 7, 9, 11). These experiments were conducted for the removal of metronidazole at an initial concentration of 10 ppm, utilizing 0.04 grams of the nanostructure, and an irradiation time of 120 minutes. The results indicate that the highest removal efficiency for Metronidazole was observed at pH 9 (80% dye removal) (Fig. 3).

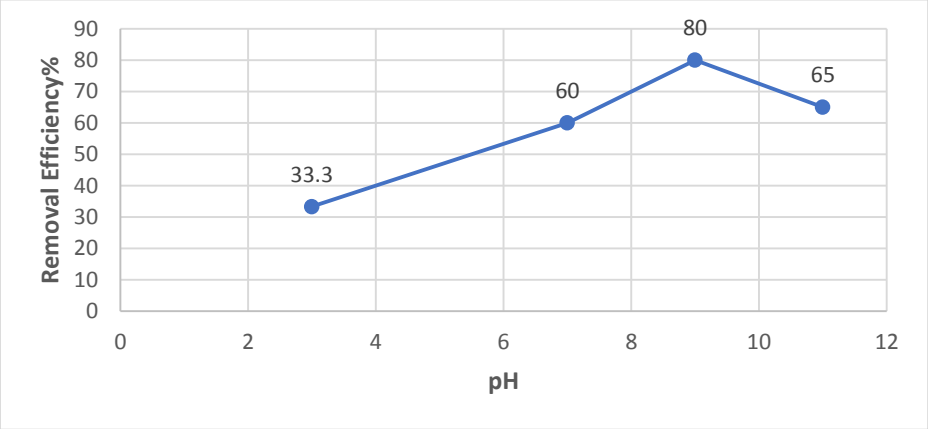

Fig. 3: Effect of pH on the metronidazole removal

3.4 Effect of contact time

The effects of contact time on Metronidazole removal at different concentrations are illustrated in Fig. 4 . These experiments were conducted with an initial concentration of 10 ppm, 0.04 grams of nanostructure, and pH 9. Based on the findings, the percentage of dye removal increased with longer contact times. At 120 minutes, the dye removal rate stabilized at approximately 60%, leading to the selection of this duration as the irradiation time (Fig. 4).

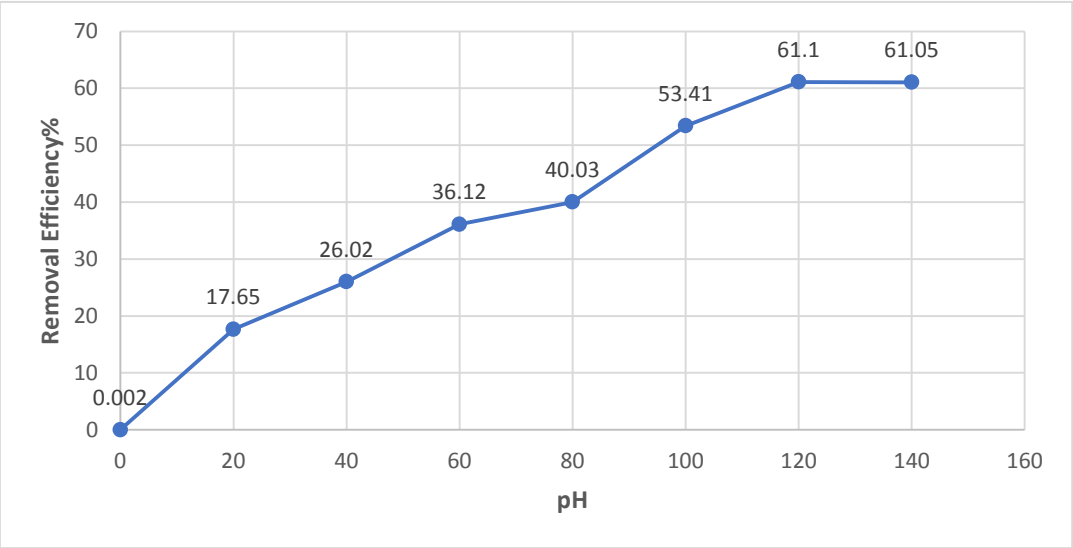

Fig. 4. Effect of contact time on the Metronidazole removal

3.5 Effect of different concentrations on dye removal

Results from experiments on Metronidazole removal, considering variables such as a contact time of 120 minutes, pH of 9, and absorbent dose of 0.04 g, revealed that dye removal decreased with increasing dye concentrations. The optimum dye removal occurred at a 10 ppm dye concentration, with an 80% removal rate (Fig. 5). In this figure, the lowest dye removal percentage (55%) was observed at the 40 ppm concentration. The decrease in removal efficiency can be explained by the limited number of active sites on the adsorbents, which would have become saturated at certain concentrations.

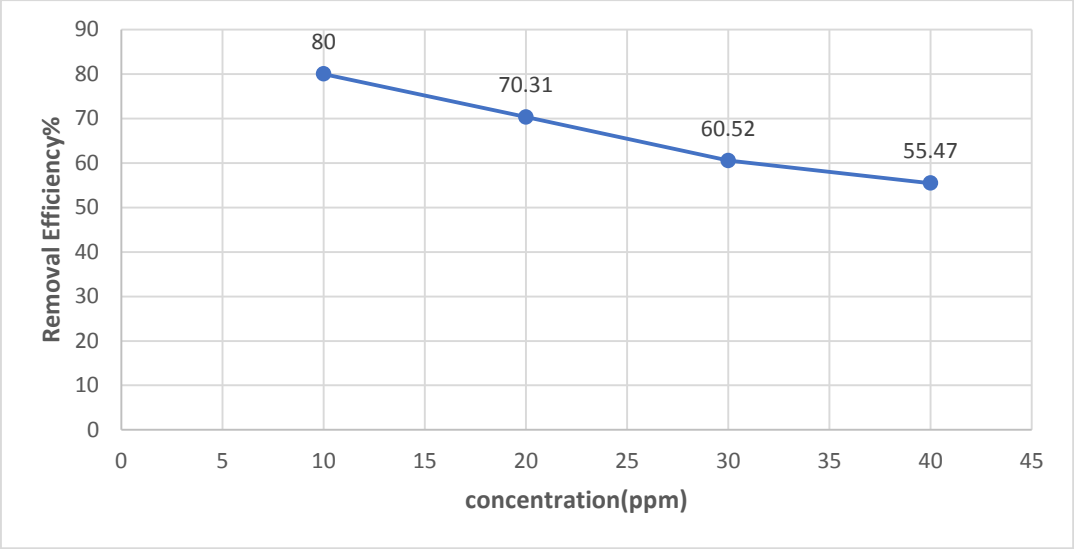

Fig. 5. Effect of different Metronidazole dye concentrations

3.6 Effect of adsorbent dose on dye removal

The adsorption of dye on the absorbent was studied by varying the quantity of adsorbent from 0.01 to 0.04g/100 ml in the test solution while maintaining the initial dye concentration at 10 mg/l, temperature at 25 ºC, pH at 9, and contact time at 120 min. As depicted in Fig. 6 , as the absorbent dose increased, the removal percentage also increased . The highest removal values were observed at an absorbent dose of 0.04 g, with approximately 99% for metronidazole .

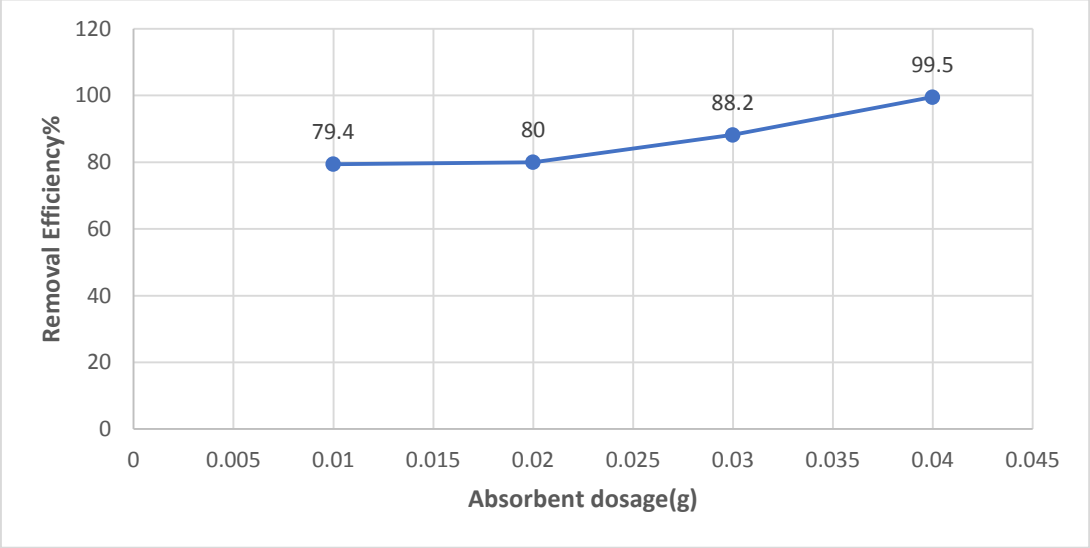

Fig .6. Effect of different absorbent doses on removal of metronidazole

3.7. Effect of temperature on dye removal

To investigate the impact of temperature, experiments were conducted on the adsorbent at temperatures ranging from 20 to 40 ºC. It was noted that the nanostructure removed 39 to 43% of metronidazole, Equilibrium was reached at 40 ºC for both dyes when treated with the nanocomposite adsorbent.

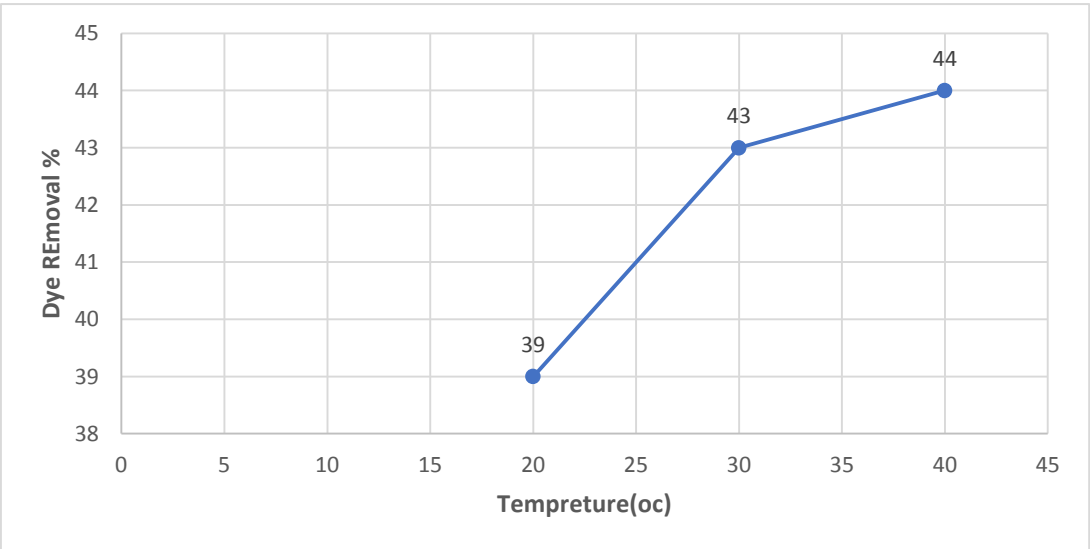

Fig .7. Effect of different temperatures on the removal of metronidazole

Based on this plot, increasing the catalyst mass improves the efficiency of dye removal. As the catalyst mass increases, more active sites become available, resulting in a higher percentage of dye removal. Conversely, reducing the color concentration decreases the removal percentage. This is because, at lower dye concentrations, the ratio of dye molecules to catalyst is low, causing most dye molecules to adhere to the catalyst surface and be removed from the solution, consequently increasing the dye removal percentage.

3.7 Adsorption Isotherm

Studying isotherms is crucial for determining the adsorption capacity of different adsorbents. To establish the adsorption isotherm, two equilibrium isotherms, namely Langmuir and Freundlich, were employed to analyze experimental data in adsorption studies. These isotherms help in comprehending the magnitude and efficiency of adsorption.

Langmuir Isotherm

The Langmuir theory assumes that adsorption is restricted to the formation of a monolayer coverage of adsorbate on a homogeneous adsorbent surface. The Langmuir equation is provided below:

$$C_e / q_e = 1/k_a V_m + C_e / V_m \qquad (1)$$

Where *qe* is the amount adsorbed per mass of adsorbent (mg/g), *Ce*is the concentration of the dye solution at equilibrium (mg/l), and *K* and *Vm* are Langmuir constants. *Vm* and *Ka* are Langmuir constants associated with the capacity and energy of adsorption, respectively. The values of *Vm* and *Ka* shown in Table 1 were determined from slopes and intercepts presented in fundamental characteristics of the Langmuir isotherm can be described by a dimensionless constant (equilibrium parameter R_L) defined by the following equation.

$$R_L = 1/ (1+K_a C_o) \qquad (2)$$

R_L values	Adsorption

R_L >1	Unfavorable
R_L =1	Linear
0< R_L <1	favorable
R_L =0	Irreversible

The correlation coefficient values of R^2 = 0.99 and R^2 = 0.84 for metronidazole obtained from the Langmuir expression suggest that the Ferundlich isotherm exhibited superior linearity.

Freundlich Isotherm

Huízar-Félix et al. reported the removal of Tetracycline pollutants by adsorption using α-Fe_2O_3 nanoparticles, indicating a good fit with the Freundlich Isotherm model. Conversely, the adsorption isotherm for α-Fe_2O_3/RGO demonstrates a better fit with the Langmuir model. The Freundlich model is predicated on the assumption that multilayer adsorption takes place on a heterogeneous adsorption surface with unequally available sites of varying adsorption energies, as described by equation 3.

$$\log q_e = \log K + 1/n \log C_e \quad (3)$$

Where *qe* is the amount of adsorbed mass (mg/g), *Ce* is the concentration of the dye solution at equilibrium (mg/l), *Kf* and 1/*n* are Freundlich constants associated with the adsorption capacity and adsorption intensity of the adsorbent, respectively. The values of *Kf* and 1/*n* are determined from the slope intercepts provided in Table 4. The results indicate *n* values of (n=2.6075 and n=2.940), suggesting significant adsorption of both dyes. This aligns well with the findings related to the R_L value.

Table. 2: Equations and results of isotherms calculations

Isotherm	Parameter	Metronidazole
Langmuir: $C_e/q_e = (1/K_aV_m) + C_e/V_m$ C/q=1/bqm+C/qm	R^2	0.9805
	b(L/mg)	0.0608
	V_m(mg/g)	1.81917
	R_L	0.5675
Freundlich: $\ln q_e = \ln K_F + (1/n) \ln C_e$	R^2	0.9812
	K_f(mg/g)	0.9786
	n	0.748

The correlation of the experimental data with the Langmuir and Freundlich isothermal models was examined using correlation coefficients. When comparing the correlation coefficient values of the Langmuir isotherm (R^2=0.980) and Freundlich isotherm (R^2=0.847) for Metronidazole, it became evident that the Freundlich isotherm provided a better fit to the data obtained in this study for these organic dyes. Additionally, the adsorption of these dyes on the nano adsorbent was determined to be a multilayer process, with evenly distributed active sites on the adsorbent surface.

Given the effective performance of nanoabsorbent in dye removal, its ease of separation from aqueous solutions, and its high activity stability over multiple cycles (five cycles), it can serve as a proficient adsorbent for water and wastewater treatment without the need for additional filtration or centrifugation. Moreover, it could serve as a viable alternative to activated carbon. The adsorption intensity parameter n was calculated to be 0.74 and 1.14 for metronidazole . From Table 2, the b value suggests that the amount of Metronidazole adsorbed per unit weight of the nanostructure.

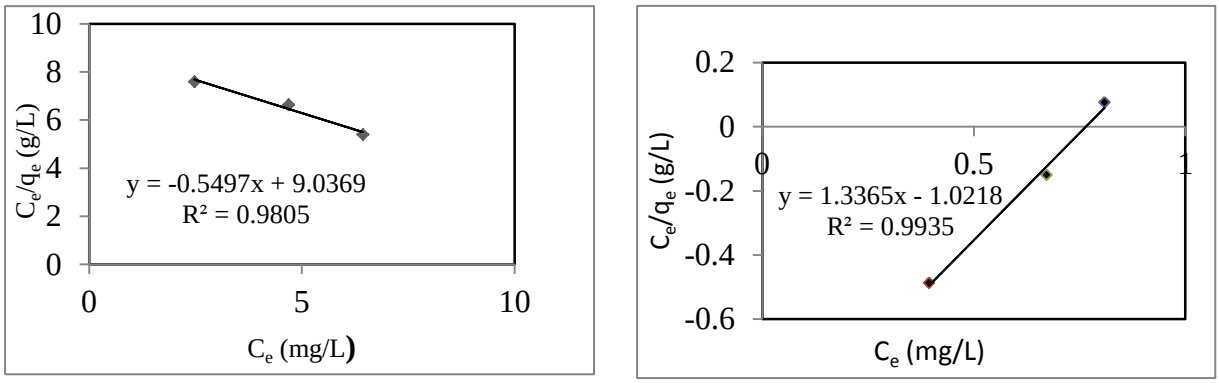

Fig.8. Langmuir (left) and Freundlich (right) isotherm plot for metronidazole dye adsorption

4.Conclusion

Nano MOF typically exhibits a limited capacity for removing anionic dyes. However, the current study demonstrated a significant enhancement in the dye removal capacity of nano MOF by surface modification with nanoparticles, synthesized successfully in this study, served as an effective adsorbent for eliminating Metronidazole from aqueous solutions. The adsorption of Metronidazole onto the nanocomposite increased with higher adsorbent doses and prolonged contact times.

nanostructures offer advantages such as natural and eco-friendly properties, availability, cost-effectiveness, biodegradability, and renewability, making it suitable for the removal of dyes like metronidazole from aqueous solutions. The experimental results aligned well with the Freundlich adsorption isotherms. The adsorption process was influenced by factors such as pH, initial dye concentration, adsorbent dose, contact time, and temperature.

The findings suggest that the employed adsorbent holds significant potential for dye removal. The research results underscored the efficiency of nano MOF as an adsorbent for eliminating metronidazole. Experiments were conducted to evaluate the impact of pH, sonication time, dye concentration, and catalyst on the adsorption process. Adsorption, a cheap and effective method, showed excellent results for dyes discussed in the study without producing any waste. Removal efficiency has been significantly increased using the adsorption technique.

Different factors greatly influence the adsorption capacity, such as absorbance, pH, time, temperature, concentration, and dose of the adsorbent. Spectrophotometric analysis suggested that treated zeolite composite material had better removal efficiency than pure zeolite.

The results of the current study highlighted the efficiency of this nanostructure as an adsorbent for removing metronidazole. Experiments were conducted to optimize parameters such as pH, contact time, dye concentration, and catalyst mass. The isotherm model was utilized to predict dye removal efficiency and was subsequently analyzed. The results (R^2 = 0.99) indicated that the Freundlich model was suitable for the empirical data. optimized values for metronidazole removal were pH: 9, contact time: 120 minutes, dye concentration: 10 mg l^{-1}, and catalyst mass: 0.04 g. Under these optimal conditions, the maximum removal efficiency reached 99.5%.

Acknowledgment

The authors thank Islamic Azad University, Ahvaz Branch for their valuable help and support.

References

[1] M. Mazloum, M. Salavati Niassary, M. K. Amini, *Sens. Actuators B* 82 (2002) 259-268.

[2] M. Shamsipur, M. R. Ganjali, A. Rouhollahi, A. Moghimi, *Anal. Chim. Acta* 434 (2001) 23-31.

[3] E. Bakker, P. Bühlmann, E. Pretsch, *Chem. Rev.* 97 (1997) 3083-3094.

[4] V. Alexander, *Chem. Rev.* 95 (1995) 273-287.

[5] K. Byriel, K. R. Dunster, L. R. Gahan, C. H. L. Kennard, J. L. Latten, I. L. Seann, P. A. Duckworth, *Inorg. Chim. Acta* 205 (1993) 191-198.

[6] K. Byriel, K. R. Dunster, L. R. Gahan, C. H. L. Kennard, J. L. Latten, I. L. Seann, P. A. Duckworth, *Polyhedron* 11 (1992) 1205-1212.

[7] V. K. Gupta, A. K. Singh, S. Mehtab, B. Gupta, *Anal. Chim. Acta* 566 (2006) 5-12.

[8] M. R. Ganjali, T. Poursaberi, M. khoobi, A. Shafiee, M. Adibi, M. Pirali-Hamedani, P. Norouzi, *Int. J. Electrochem. Sci*. 6 (2011) 717-724.

[9] Y. Umezawa, K. Umezawa, H. Sato, *Pure Appl. Chem*. 67 (1995) 507-512.

[10] R. P. Buck, E. Lindner, *Pure Appl. Chem.* 66 (1994) 2527-2531.

[11] E. L. Jammal A. Bouklouze A. A. Patriarche, *Talanta*, 38 (1991) 929-935.

[12] M. Yi-long, R. Xiao-hong, Z. Shi-ming, *J. Tongji Medical Uni.* 12 (1992) 98-102.

[13] A. Kumar, S. K. Mittal, *Sens. Actuators B* 99 (2004) 340-343.

[14] A. Kumar, M. Sameena, *Sens. Actuators B* 123 (2007) 429-436.

[15] M.S. Thomas, S. Thomas, L.A. Pothen, Science and Technology of Nanomaterials: Introduction, in: Nanotechnol. Environ. Remediat., John Wiley & Sons, Ltd, 2022: pp. 1–15.

[16] L. Qi, Z. Xu, X. Jiang, C. Hu, X. Zou, Carbohydr. Res. 339 (2004) 2693–2700.

[17] C. Yao, Y. Shin, L.-Q. Wang, Windisch Charles F., W.D. Samuels, B.W. Arey, C. Wang, Risen William M., G.J. Exarhos, J. Phys. Chem. C. 111 (2007) 15141–15145.

[18] N. Baccile, G. Laurent, F. Babonneau, F. Fayon, M.-M. Titirici, M. Antonietti, J. Phys. Chem. C. 113 (2009) 9644–9654.

[19] A. Gedanken, Using sonochemistry for the fabrication of nanomaterials, 11 (2004) 47–55.

[20] S. Barcikowski, A. Plech, K.S. Suslick, A. Vogel, MRS. Bull. 44 (2019) 382–391.

[21] G. Qiu, Q. Wang, M. Nie, Macromol. Mater. Eng. 291 (2006) 68–74.

[22] G. Song, S. Ma, G. Tang, X. Wang, Eng. Asp. 364 (2010) 99–104.

[23] H. Xia, Q. Wang, J. Nanoparticle Res. 3 (2001) 401–411.

[24] M. Hosseini, H. Rezaei Ashtiani, D. Ghanbari, Ultrasonic Preparation of Cobalt, Nickel, J. Nanostructures. 12 (2022) 588–597.

[25] J. Sun, L. Qian, J. Li, Polymer (Guildf). 210 (2020) 122994.

[26] X. Wang, T. Chen, J. Hong, W. Luo, B. Zeng, C. Yuan, Y. Xu, G. Chen, L. Dai, Compos. Part B Eng. 200 (2020) 108271.